

Computational Model of Nitrogen Vibrational Relaxation by Electron Collisions

John D. Mertens*

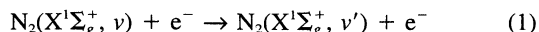
Trinity College, Hartford, Connecticut 06106

Nitrogen vibrational relaxation by electron collisions has been studied by developing a complete vibrational state-to-state rate coefficient database for electron temperatures of 0.1–5.0 eV. This database was used to model a wide range of N_2 -e vibrational relaxation processes by solving and numerically integrating the master equation with respect to time. These results were used to develop a simple set of equations that accurately model nitrogen vibrational relaxation by electron collisions for electron and nitrogen vibrational temperatures ranging from 0.0 to 5.0 eV. The results are presented in the form of polynomial equations that could be easily incorporated into numerical models of more complex systems.

Introduction

THE importance of including accurate descriptions of molecular vibrational relaxation processes in numerical models of highly nonequilibrium flowfields has been explained by many investigators.^{1–7} For example, the molecular vibrational temperatures downstream of the shock waves of hypersonic vehicles play an important role in determining the radiative heat transfer load of such vehicles. In the cases where flow conditions result in significant ionization of the gases, electron–molecule collisions are much more frequent than molecule–molecule collisions, because of the small mass and high velocities of the electrons. Free electrons can also travel through the shock wave and collide with cold molecules upstream of the shock wave. Therefore, in these ionized flows, where there is a significant difference between electron translational temperatures and molecular vibrational temperatures, this mechanism of energy transfer must be included in flow-field models.^{1–7} The goal of the present work is to determine the rate of nitrogen vibrational relaxation from electron collisions for any vibrational and electron temperatures, and to use the results to provide a simple and accurate model of the process that will be easily incorporated into numerical models of nonequilibrium hypersonic flows.

The interactions of electrons and nitrogen molecules have been considered in many studies.^{2–9} Four of the studies^{4–7} that are particularly relevant to the present work look directly at vibrational transitions of electronic-ground-state nitrogen as a result of electron collisions:



where the rate of change of the number density of N_2 molecules in vibrational state v is given by the master equation:

$$\frac{dN_v}{dt} = N_e \sum_{v'=0}^m (k_{v',v} \times N_{v'} - k_{v,v'} \times N_v) \quad (2)$$

m is the maximum vibrational quantum number. The effects of molecular dissociation on vibrational relaxation are negligible over the range of vibrational temperatures in this study; hence, dissociation is neglected in Eq. (2).

Huo et al.⁴ performed ab initio calculations of N_2 cross sections for reaction (1) and tabulated state-to-state rate coefficients ($k_{v',v}$) for electron temperatures of 0.1–5.0 eV; initial vibrational quantum numbers of $v = 0–12$; and changes in vibrational states ($\Delta v = v' - v$) of -5 to $+5$, for N_2 rotational quantum numbers of $J = 0, 50$, and 150 . Huo et al.'s work⁴ expanded and corrected previous compilations that were derived from experimental measurements with a factor-of-2 error. With the corrections, the results of Huo et al. are in very good agreement with available experimental results.

Lee^{5,6} performed two studies of nitrogen vibrational relaxation by electron impact. In the 1986 study,⁵ approximate values of N_2 cross sections for reaction (1) were computed using a semiempirical method and an approximate potential function.⁵ Values of $k_{v',v}$ were tabulated for vibrational transitions from the ground state ($v = 0$) to final states of $v' = 1$ to 10 at electron temperatures of 0.1–5.0 eV. Lee then used these rate coefficients and an analytical method involving the diffusion model¹⁰ to obtain the time variation of total nitrogen vibrational energy per unit volume for fixed electron temperatures. These solutions were used to determine a defined nitrogen vibrational relaxation time for electron temperatures between 0.1 and 5.0 eV. This analysis relied on several major simplifications and assumptions that would make the results very approximate.^{5,10} The results of Lee's 1992 vibrational relaxation study⁶ were much improved, and only the 1992 results will be presented here for comparison and discussion.

In the 1992 study, Lee⁶ employed an approximate computational solution of the master equation for reaction (1) to determine instantaneous N_2 vibrational relaxation times for vibrational temperatures of $T_v = 0.1–0.5$ eV and electron temperatures of $T_e = 0.1–5.0$ eV. A harmonic oscillator model and Boltzmann vibrational level distributions were assumed to calculate both E_v and E_v^* . E_v is the total N_2 vibrational energy per unit volume at T_v . E_v^* is the total N_2 vibrational energy per unit volume that would be present if the vibrational temperature reached equilibrium with a fixed electron temperature, i.e., $T_v = T_e$. The rate coefficient database of Huo et al.⁴ for initial vibrational quantum numbers of $v = 0–12$, a rotational quantum number of $J = 50$, and vibrational transitions of $\Delta v = -5$ to $+5$ was extended to include vibrational transitions of up to $\Delta v = \pm 10$, using an Arrhenius curve fit.⁶ Lee⁶ then considered only transitions between the 0 through 12 vibrational quantum levels, i.e., $v = 0–12$ and $v' = 0–12$, with Δv up to ± 10 , to compute approximate values of dE_v/dt using the master equation and harmonic oscillator vibrational energy levels for fixed values of T_v and T_e . Instantaneous vibrational relaxation times

Received Jan. 15, 1998; revision received Aug. 4, 1998; accepted for publication Nov. 30, 1998. Copyright © 1999 by the American Institute of Aeronautics and Astronautics, Inc. All rights reserved.

*Associate Professor of Engineering.

were then calculated as functions of T_v and T_e using the equation

$$\tau = \frac{(E_v^* - E_v)}{\left(\frac{dE_v}{dt}\right)} \quad (3)$$

Results for $p_e\tau$ (atm-s, where p_e is electron pressure) were plotted for vibrational temperatures of 0.1–0.5 eV and electron temperatures of 0.1–5.0 eV. However, the accuracy of these results decreases rapidly as electron and vibrational temperatures increase as a result of two factors: as T_e and T_v increase, transitions to vibrational quantum levels above $v' = 12$ become significant, and the use of the harmonic oscillator model to compute E_v^* becomes highly inaccurate at high electron temperatures. Similar problems would also develop if this technique were to be used to calculate relaxation times for vibrational temperatures above 0.5 eV, as initial vibrational quantum levels above $v = 12$ would become populated.

Hansen⁷ developed nitrogen vibrational relaxation times for reaction (1) using essentially the same technique as Lee.⁶ Hansen used the rate coefficients of Lee⁵ to expand the rate coefficient database of Huo et al.⁴ to include transitions of Δv up to +7. Hansen then used these rate coefficients and harmonic-oscillator-model vibrational energy levels to calculate relaxation times defined by Eq. (3) for electron temperatures of 0.3–5.0 eV. Although not stated explicitly, Hansen's results are apparently for vibrational-ground-state nitrogen ($T_v \approx 0$). As expected, Hansen's results agree well with Lee.⁶ They also have the same inaccuracy at high electron temperatures because of the use of the harmonic oscillator model to compute E_v^* .

Methodology of the Current Study

In the present study, the rate coefficient database of Huo et al.⁴ for $J = 50$ was expanded to include all transitions between vibrational quantum levels 0–50 for electron temperatures of 0.1–5.0 eV, using empirical and curve-fitting methods that are described next. Dissociation was not considered. These rate coefficients were used to calculate time histories of all N_2 -vibrational-level populations for a wide variety of conditions by integrating the master equation numerically:

$$N_v(t + \Delta t) = N_v(t) + \left[\frac{dN_v}{dt}(t)\right] \times \Delta t \quad (4)$$

Nitrogen vibrational energy levels from Huber and Herzberg¹¹ were used to compute N_2 partition functions and initial Boltzmann vibrational level distributions. Time-step values (Δt) were computed for each run using Eq. (5):

$$\Delta t = \left| \frac{N_M}{\left(\frac{dN_{v=0}}{dt}\right)_{t=0}} \right| \times 10^{-3} \quad (5)$$

N_M is the total nitrogen number density. Reducing the arbitrary time-step multiplying factor in Eq. (5) below 10^{-3} did not make any significant difference in the resolution of the calculations.

This technique can be used to determine time histories of nitrogen-vibrational-level populations for any initial nitrogen-vibrational-level distribution and any prescribed time histories of electron temperature, electron number density, or total nitrogen number density. This is demonstrated in Fig. 1, in which a total energy balance is assumed, i.e., any energy transfer to or from N_2 vibrations is removed or added to total electron translational energy, for fixed electron and nitrogen number densities, and electron and vibrational temperatures are allowed to change. (Figure 1 will be discussed further in the

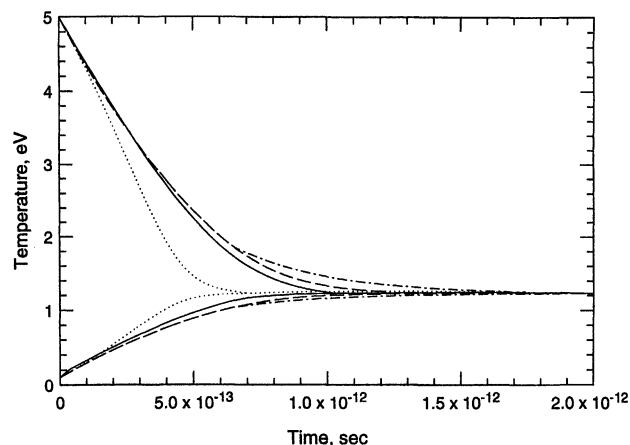


Fig. 1 Computed results for N_2 -e vibrational relaxation with overall energy balance. Initial temperature: $T_e = 5.0$ eV, $T_v = 0.1$ eV, $N_M = 1.0 \times 10^{21}/\text{cm}^3$, and $N_e = 3.0 \times 10^{20}/\text{cm}^3$. —, complete rate constant database; ---, Eqs. (11–13); ···, Eqs. (11–14); and ···, Lee.⁶

Vibrational Relaxation Results section.) However, this computational technique utilizes a large rate constant database and requires significant computational time. The goal of the present study is to use this technique to determine instantaneous vibrational relaxation times as defined by Eq. (3) for all electron and vibrational temperatures and to consolidate the results into a simple set of equations. These results can be used to determine the relaxation of any N_2 -e system using a relatively simple computational method.

These values of instantaneous vibrational relaxation times were determined by performing calculations with electron temperature, electron number density, and total nitrogen number density held constant for each computational run. E_v was calculated at each time step by summing the vibrational energy per unit volume of each vibrational quantum level using nitrogen vibrational energy levels $\varepsilon(v)$ from Huber and Herzberg¹¹:

$$E_v = \sum_{v=0}^m \varepsilon(v) \times N_v \quad (6)$$

E_v^* was calculated using Eq. (6) and Boltzmann vibrational level distributions at the fixed electron temperature. dE_v/dt was calculated at each time step by summing the rate of change of vibrational energy per unit volume of each vibrational quantum level using the master equation:

$$\frac{dE_v}{dt} = \sum_{v=0}^m \varepsilon(v) \times \frac{dN_v}{dt} \quad (7)$$

Instantaneous values of $N_e\tau$ were calculated by multiplying both sides of Eq. (3) by electron number density:

$$N_e\tau = N_e \times \frac{(E_v^* - E_v)}{\left(\frac{dE_v}{dt}\right)} \quad (8)$$

It can be seen from examining Eqs. (2–8) that $N_e\tau$ is independent of total nitrogen number density and electron number density during each run, and that it is only a function of T_e and the instantaneous relative population distribution of the vibrational quantum levels. This makes it possible to determine values of $N_e\tau$ for all vibrational and electron temperatures by performing runs at fixed electron temperatures of 0.1–5.0 eV at 0.1 eV increments.

Effective nitrogen vibrational temperatures were determined during each run by comparing the instantaneous value of E_v

to the vibrational energy that would result from an equivalent Boltzmann vibrational temperature. Values of $N_e\tau$ were determined over the course of each run at effective vibrational temperature increments of 0.1 eV. Each run was begun with an initial vibrational temperature of 0.0 eV, and was halted when values of E_v were within 1% of E_v^* . Computational runs were performed for fixed electron temperatures ranging from 0.1 to 5.0 eV at increments of 0.1 eV. This provided values of $N_e\tau$ for temperature ranges of $0.1 \text{ eV} \leq T_e \leq 5.0 \text{ eV}$, and $0.0 \text{ eV} \leq T_v < T_e$.

This same technique for computing instantaneous vibrational relaxation times [Eqs. (1–8)] was also used to determine $N_e\tau$ as a function of T_v and T_e by simply assuming instantaneous Boltzmann vibrational level distributions at any value of T_v . This will be discussed further in the Vibrational Relaxation Results section.

Expansion of Rate Coefficient Database

Each table of rate coefficients from Huo et al.⁴ for $J = 50$, and a particular electron temperature was expanded to include all transitions between vibrational quantum levels 0–50, using a series of three steps.

Step 1

Huo et al.'s⁴ rate coefficients for N_2 excitation transitions with the same Δv but different initial quantum levels were used to calculate the rate coefficients for all transitions with that value of Δv . An Arrhenius rate coefficient expression was used to compute the pre-exponential constant $A_{v,v'}$ for each of Huo et al.'s⁴ rate coefficients:

$$k_{v,v'} = A_{v,v'} \exp\{[\varepsilon(v) - \varepsilon(v')]/kT_e\} \quad (9)$$

These values of $A_{v,v'}$ were curve fit as a function of v for transitions with a particular Δv , and used to project the value of $A_{v,v'}$ for other transitions with the same value of Δv . These values of $A_{v,v'}$ were then used in Eq. (9) to calculate $k_{v,v'}$ for those transitions. Figure 2 shows the results for $\Delta v = +1$ to $+5$ for $T_e = 3.0 \text{ eV}$.

Step 2

Step 1 provided rate coefficients for all transitions with $\Delta v = +1$ to $+5$. These rate coefficients were expanded to include all Δv greater than $+5$, using a linear curve fit of a semilog plot of k vs Δv for each initial quantum level. Figure 3 shows the results for initial vibrational quantum numbers of 0, 10, 20, 30, and 40 for $T_e = 3.0 \text{ eV}$. This technique results in large uncertainties of k for large values of Δv . However, the rate coefficients for these transitions are small, and play a very

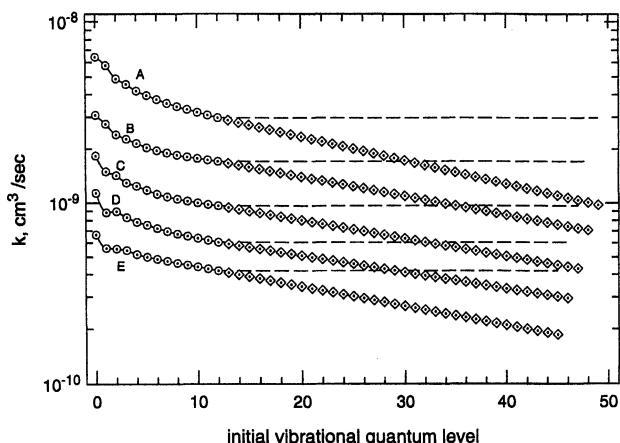


Fig. 2 Extension of rate coefficient database for fixed Δv at $T_e = 3.0 \text{ eV}$. \odot , Huo et al.⁴; \diamond , this work; A, $\Delta v = +1$; B, $\Delta v = +2$; C, $\Delta v = +3$; D, $\Delta v = +4$; E, $\Delta v = +5$; and ---, limits that were used in uncertainty analysis.

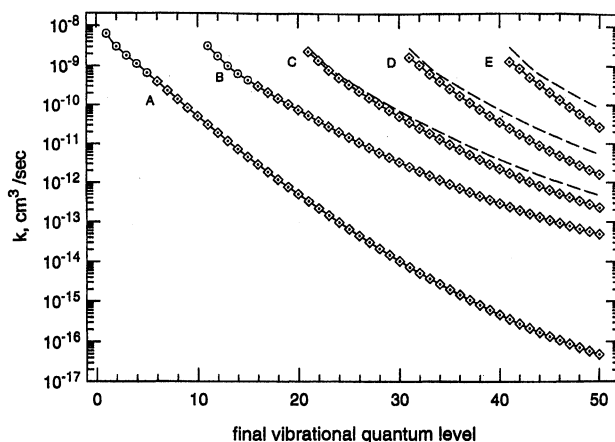


Fig. 3 Extension of excitation rate coefficient database for fixed initial vibrational quantum numbers at $T_e = 3.0 \text{ eV}$. \odot , Huo et al.⁴; \diamond , this work; A, $v_{in} = 0$; B, $v_{in} = 10$; C, $v_{in} = 20$; D, $v_{in} = 30$; E, $v_{in} = 40$; and ---, limits that were used in uncertainty analysis.

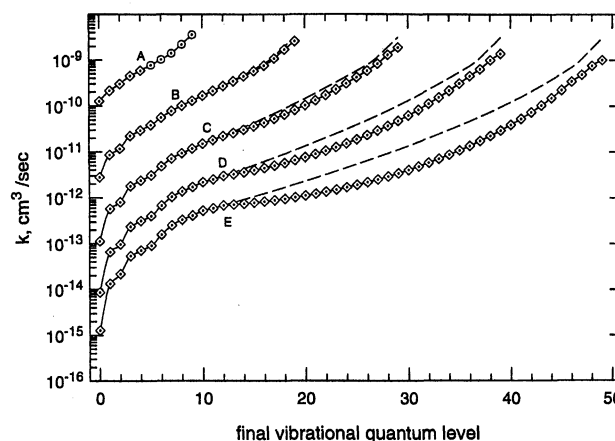


Fig. 4 De-excitation rate coefficients at $T_e = 3.0 \text{ eV}$. \odot , Huo et al.⁴; \diamond , this work; A, $v_{in} = 10$; B, $v_{in} = 20$; C, $v_{in} = 30$; D, $v_{in} = 40$; E, $v_{in} = 50$; and ---, limits that were used in uncertainty analysis.

small role in the calculations. This is discussed in more detail in the uncertainty analysis of the results.

Step 3

Steps 1 and 2 provided values of k for all N_2 excitation transitions, at each electron temperature. These excitation rate coefficients were used to calculate values of all de-excitation rate coefficients that were not included in the database of Huo et al.⁴ using detailed balancing¹:

$$k_{v',v} = k_{v,v'} \times N_v^*/N_{v'}^* \quad (10)$$

Values of N_v^* and $N_{v'}^*$ were calculated using Boltzmann vibrational temperature distributions at the electron temperatures. Figure 4 shows de-excitation rate coefficients for initial vibrational quantum numbers of 10, 20, 30, 40, and 50 for $T_e = 3.0 \text{ eV}$.

This three-step method was used to expand the rate coefficient database of Huo et al.⁴ at each electron temperature ($T_e = 0.1$ – 5.0 eV at 0.1 eV increments), resulting in a $51 \times 51 \times 50$ three-dimensional array of rate coefficients: $k_{v,v'}$ ($v = 0$ – 50 , $v' = 0$ – 50 , $T_e = 0.1$ – 5.0 eV).

Vibrational Relaxation Results

Figure 5 shows sample results of nitrogen vibrational excitation used to determine $N_e\tau$ at five fixed electron temperatures ranging from 1.0 to 5.0 eV. Time histories of effective vibrational temperature are shown as a function of $N_e \times t$ (electron

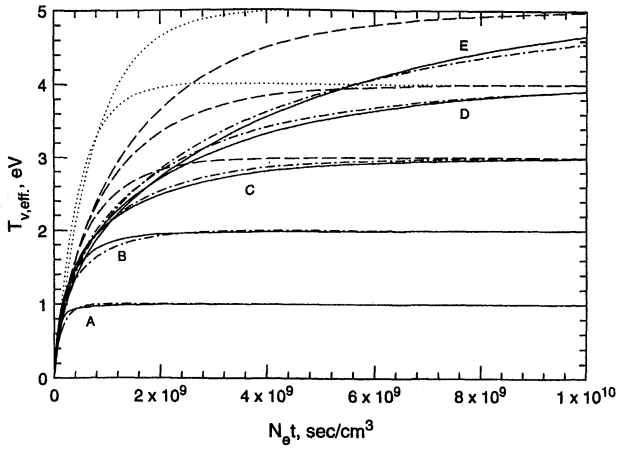


Fig. 5 Computed results for nitrogen vibrational relaxation for fixed electron temperatures. A, $T_e = 1.0$ eV; B, $T_e = 2.0$ eV; C, $T_e = 3.0$ eV; D, $T_e = 4.0$ eV; and E, $T_e = 5.0$ eV. —, complete rate constant database; ---, (C, D, and E only) Eqs. (11–13); ···, Eqs. (11–14); and ···, (D and E only) Lee.⁶

number density multiplied by time), which results in curves that are independent of electron number density. It should be noted that $N_e \times t$ is a measure of elapsed or reaction time, and is a completely different quantity from $N_e \tau$, which is a measure of relaxation rate, as defined by Eq. (8). The curves of effective vibrational temperature are also independent of total nitrogen number density, which is a result of holding electron temperature, electron number density, and total nitrogen number density constant during each run, as discussed previously. The coordinates and slope of each point on the curves can be used to determine $N_e \tau$ at that value of T_e and $T_{v,eff}$, using Eq. (8). Figure 6 shows computed instantaneous vibrational population distributions for the case of $T_e = 3.0$ eV at four effective vibrational temperatures, and compares them with Boltzmann population distributions. This shows that, as the relaxation process proceeds, a middle range of vibrational levels becomes populated above Boltzmann levels, whereas the upper vibrational levels remain below Boltzmann levels until very late in the relaxation process. Figure 6 also shows that eventually this bubble effect smooths out and a Boltzmann distribution at $T_v = T_e$ is reached. This phenomenon is due to the fact that, for a given T_e and Δv , Huo et al.'s⁴ results show that the ratio of an excitation rate coefficient with a lower initial vibrational level ($v = 0-2$) and an excitation rate coefficient with a higher initial vibrational level ($v = 3-5$) is greater than the ratio of the Boltzmann populations of the two initial vibrational levels at T_e (see Fig. 2). This is a result of resonant electron impact at the lower initial vibrational levels.^{2,4} This also results in proportionately larger de-excitation rate coefficients for lower initial vibrational levels. This results in lower vibrational states becoming populated more quickly than upper vibrational states relative to Boltzmann distribution levels, and also delays the distribution of vibrational energy to the upper levels. This phenomenon persists even when radical changes are made in the rate coefficient database, and is discussed in more detail in the uncertainty analysis. It should be noted that the significance of this effect would decrease in flowfield conditions for which other vibrational relaxation processes are significant, or in which electron temperatures are changing rapidly.

Figure 7 shows the results for $N_e \tau$ determined from the preceding computational runs and from assuming instantaneous Boltzmann vibrational population distributions, as mentioned previously. It can be seen that the deviation from Boltzmann distributions during the relaxation process for fixed electron temperatures results in significantly larger relaxation times for effective vibrational temperatures above 1.0 eV. This is a result of the bubble effect at higher effective vibrational temperatures delaying energy transfer to higher vibrational quantum levels

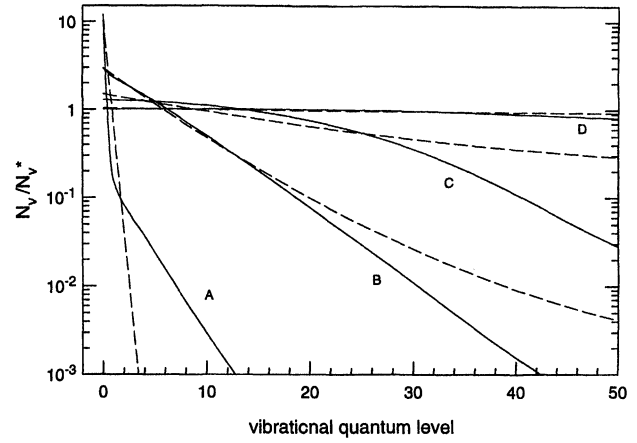


Fig. 6 Vibrational quantum level population distributions at various effective vibrational temperatures for case C of Fig. 5. —: A, $T_{v,eff} = 0.1$ eV; B, $T_{v,eff} = 1.0$ eV; C, $T_{v,eff} = 2.0$ eV; and D, $T_{v,eff} = 2.9$ eV. ---, Boltzmann population distributions at equivalent vibrational temperatures.

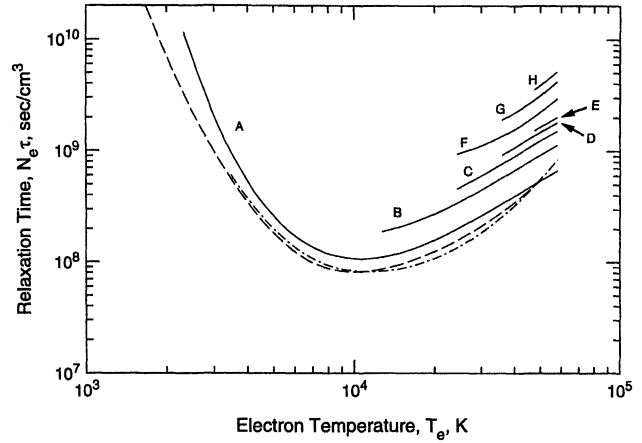


Fig. 7 Instantaneous nitrogen vibrational relaxation times as a function of electron and nitrogen vibrational temperatures. —, this work; A, $T_v = T_{v,eff} = 0.0$ eV; B, $T_v = T_{v,eff} = 1.0$ eV; C, $T_v = 2.0$ eV; D, $T_v = 3.0$ eV; E, $T_v = 4.0$ eV; F, $T_{v,eff} = 2.0$ eV; G, $T_{v,eff} = 3.0$ eV; and H, $T_{v,eff} = 4.0$ eV. ---, results of Lee⁶; and ···, results of Hansen.⁷

and reducing the instantaneous value of dE_v/dt in Eq. (8). This effect generates two different sets of results for instantaneous vibrational relaxation: $N_e \tau$ as a function of electron temperature and Boltzmann vibrational temperature, and $N_e \tau$ as a function of electron temperature and effective vibrational temperature during a relaxation process with fixed T_e starting at $T_v = 0.0$ eV. Least-squares polynomial fits to these two sets of results are given next, with a maximum deviation of $\pm 3\%$ from the results.

1) For Boltzmann vibrational temperatures (also for $T_{v,eff} \leq 12,000$ K),

$$N_e \tau = 4.72 \times 10^{27} \cdot T_e^{-5} - 3.32 \times 10^{24} \cdot T_e^{-4} + 9.33 \times 10^{20} \cdot T_e^{-3} - 1.16 \times 10^{17} \cdot T_e^{-2} + 6.2 \times 10^{12} \cdot T_e^{-1}, \text{ s/cm}^3, \quad 2300 \text{ K} \leq T_e \leq 10,400 \text{ K} \quad (11)$$

$$N_e \tau = 8.97 \times 10^7 - 2190 \cdot T_e + 0.328 \cdot T_e^2 - 2.06 \times 10^{-6} \cdot T_e^3, \text{ s/cm}^3, \quad 10,400 \text{ K} < T_e \leq 58,000 \text{ K} \quad (12)$$

where Eqs. (11) and (12) should be multiplied by

$$(1 + 6.63 \times 10^{-5} \cdot T_v - 4.82 \times 10^{-10} \cdot T_v^2) \quad (13)$$

for $T_v < T_e$.

2) For effective vibrational temperatures: Results for effective vibrational temperatures below 12,000 K are fit by Eqs. (11–13). Results for effective vibrational temperatures above 12,000 K are fit by Eq. (14):

$$N_e \tau = (4.8 \times 10^8 + 1.37 \times 10^4 \cdot T_e - 8.52 \times 10^{-2} \cdot T_e^2 + 9.57 \times 10^{-6} \cdot T_e^3) \times (-6.65 \times 10^{-2} + 5.52 \times 10^{-5} \cdot T_{v,eff} - 3.18 \times 10^{-10} \cdot T_{v,eff}^2), \text{ s/cm}^3$$

$$12,000 \text{ K} < T_{v,eff} \leq 46,400 \text{ K}, \quad T_{v,eff} < T_e \leq 58,000 \text{ K} \quad (14)$$

Figure 7 also shows that the simple models of Lee⁶ and Hansen⁷ provide good agreement with the present study for $T_v = 0.0$ eV. Their results are slightly lower for electron temperatures below 4.5 eV, as their use of the harmonic oscillator model resulted in lower values for E_v^* . However, this is counteracted by limiting the range of allowed transitions, which results in lower values of dE_v/dt . This latter effect becomes more important at higher electron temperatures, and eventually produces slightly higher results for electron temperatures above 4.5 eV.

Equations (11–14) can be used to determine the rate of change of nitrogen vibrational energy caused by electron collisions at any instant in time in any system using Eq. (8). For vibrational temperatures above 1.0 eV, it would be the responsibility of the user to determine which solution set is most appropriate for a particular system. The author suggests using Eq. (14) for conditions in which the vibrational relaxation process is dominated by collisions with electrons that originate from an outside source, such as the case of electrons passing through a shock wave and interacting with unheated air.

Figures 1 and 5 show comparisons between vibrational relaxation results using the complete rate constant database, the results of Eqs. (11–14) to compute $E_v(t)$ using Eq. (8), and the results of Lee⁶ to compute $E_v(t)$ using Eq. (8). Figure 1 shows that the results using $N_e \tau$ for Boltzmann vibrational population distributions provide excellent agreement with the results of the complete rate constant database for an energy balance system. Figure 5 shows that the results using $N_e \tau$ for effective vibrational temperatures provide excellent agreement with the results of the complete rate constant database for fixed electron temperatures. The results of Lee⁶ overpredict the nitrogen relaxation rates in both cases, as they only provide values of $N_e \tau$ determined for very low vibrational temperatures. In all cases, using Eqs. (11–14) to perform the calculations uses less than 10^{-4} of the computation time and less than one-twentieth of the computer memory required when using the complete rate constant database.

Uncertainty Analysis

As mentioned previously, expansion of the rate coefficient database results in large uncertainties in the rate coefficients of some transitions. Computational runs were performed for a variety of very liberal upper and lower bounds on the rate coefficient database to determine the sensitivity of the results for $N_e \tau$ to these uncertainties. Table 1 compares the results for $T_e = 3.0$ eV and $T_{v,eff} = 0.5$ and 2.5 eV for five different databases, including the database used in the current study. Database A tests the effects of assuming a constant value for the rate constants determined in step 1 of the database expansion. This is a maximum upper limit on these rate constant values, as shown by the dashed lines in Fig. 2, resulting in as much as a factor of 3 uncertainty in values of the higher vibrational level rate coefficients. The effects of this assumed upper limit in steps 2 and 3 of the database expansion are shown by the dashed lines in Fig. 3 and 4. Databases B, C, and D examine the effects of limiting the values of Δv that are allowed in step 2 of the database expansion. This also limits the de-excitation transitions that are allowed in step 3 of the database expansion.

Table 1 Sensitivity of nitrogen vibrational relaxation to changes in rate coefficient database for electron temperature of 3.0 eV

Rate coefficient database	$T_{v,eff} = 0.5$ eV		$T_{v,eff} = 2.5$ eV	
	$N_e \tau$, s/cm ³	$N_e \tau$, s/cm ³	$N_e \tau$, s/cm ³	$N_e \tau$, s/cm ³
Current study	4.8×10^7	4.25×10^8	2.1×10^9	1.6×10^9
A	4.8×10^7	4.25×10^8	1.8×10^9	1.2×10^9
B	4.85×10^7	4.35×10^8	2.45×10^9	2.0×10^9
C	5.05×10^7	4.55×10^8	3.2×10^9	2.6×10^9
D	6.75×10^7	6.6×10^8	7.3×10^9	6.0×10^9

Databases B, C, and D limit the maximum values of Δv to ± 15 , ± 10 , and ± 5 , respectively. In other words, database B results in rate coefficients equal to zero for all transitions with $|\Delta v|$ greater than 15. This was considered the lower limit on the rate constants determined in steps 2 and 3. Databases C and D were included for additional sensitivity information.

Table 1 shows that the changes in the database did affect relaxation times and the time it took to reach $T_{v,eff}$, particularly as $T_{v,eff}$ approaches T_e . However, the population distributions at any given effective vibrational temperature were essentially identical for all five databases. This confirms that the bubble effect is not an artifact of the rate coefficient database expansion techniques.

Combining the results for databases A and B shown in Table 1, with the independent uncertainties of $\pm 10\%$ reported by Huo et al.⁴ for their results, provides a recommended total uncertainty in the results for $N_e \tau$ of $\pm 14\%$ for low values of $T_{v,eff}$, rising to $\pm 27\%$ as $T_{v,eff}$ reaches within 0.5 eV of T_e . These uncertainties also apply to the results assuming Boltzmann vibrational temperatures given by Eqs. (11–13).

Conclusions

The current study has developed results for nitrogen vibrational relaxation by electron collisions over a wide range of electron and nitrogen vibrational temperatures using a complete vibrational state-to-state rate coefficient database. The results show that vibrational population distributions deviate significantly from Boltzmann distributions during relaxation processes with fixed electron temperatures, but ultimately reach a Boltzmann distribution when reaching equilibrium. Quantitative results for instantaneous vibrational relaxation times were determined as functions of electron and nitrogen vibrational temperatures, and the results are presented in the form of polynomial equations that could be easily incorporated into numerical models of more complex systems. These equations make it possible to accurately model nitrogen vibrational relaxation by electron collisions using less than 10^{-4} of the computation time and less than one-twentieth of the computer memory required using the complete master equation.

References

- ¹Park, C., *Nonequilibrium Hypersonic Aerothermodynamics*, Wiley, New York, 1990.
- ²Huo, W. M., "Electron Collision Cross Sections Involving Excited States," *Nonequilibrium Processes in Partially Ionized Gases*, Plenum, New York, 1990, pp. 341–348.
- ³Colonna, G., and Capitelli, M., "On the Coupling of Electron and Vibrational Kinetics in the Boundary Layer of Hypersonic Flow," AIAA Paper 95-2071, June 1995.
- ⁴Huo, W. M., McKoy, V., Lima, M. A. P., and Gibson, T. L., "Electron-Nitrogen Molecule Collisions in High-Temperature Nonequilibrium Air," *Thermophysical Aspects of Reentry Flows*, edited by J. N. Moss and C. D. Scott, Vol. 103, Progress in Astronautics and Aeronautics, AIAA, New York, 1986, pp. 152–196; also AIAA Paper 85-1034, June 1985.
- ⁵Lee, J., "Electron-Impact Vibrational Excitation Rates in the Flow-field of Aeroassisted Orbital Transfer Vehicles," *Thermophysical Aspects of Reentry Flows*, edited by J. N. Moss and C. D. Scott, Vol. 103, Progress in Astronautics and Aeronautics, AIAA, New York, 1986, pp. 197–224.

⁶Lee, J., "Electron-Impact Vibrational Relaxation in High-Temperature Nitrogen," AIAA Paper 92-0807, Jan. 1992.

⁷Hansen, C., "Vibrational Relaxation in Very High Temperature Nitrogen," AIAA Paper 91-0465, Jan. 1991.

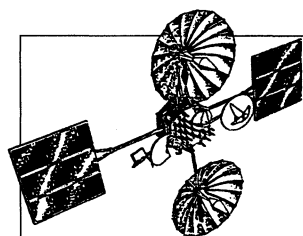
⁸Schulz, G. J., "A Review of Vibrational Excitation of Molecules by Electron Impact at Low Energies," *Principles of Laser Plasmas*, Wiley, New York, 1976, pp. 33-69.

⁹DeBenedictis, S., and Dilecce, G., "Vibrational Relaxation of $N_2(C,v)$ State in N_2 Pulsed RF Discharge: Electron Impact and Pooling

Reactions," *Chemical Physics*, Vol. 192, 1995, pp. 149-162.

¹⁰Lee, J., "Basic Governing Equations for the Flight Regimes of Aeroassisted Orbital Transfer Vehicles," *Thermal Design of Aeroassisted Orbital Transfer Vehicles*, edited by H. F. Nelson, Vol. 96, Progress in Astronautics and Aeronautics, AIAA, New York, 1985, pp. 3-53; also AIAA Paper 84-1729, June 1984.

¹¹Huber, K. P., and Herzberg, G., *Molecular Spectra and Molecular Structure, IV. Constants of Diatomic Molecules*, Reinhold, New York, 1979.



Satellite Thermal Control Handbook

David G. Gilmore, *Editor*

The Satellite Thermal Control Handbook (David G. Gilmore, Editor), published by The Aerospace Corporation Press and distributed by AIAA, is a compendium of corporate knowledge and heritage of thermal control of unmanned Earth-orbiting satellites. This practical handbook provides thermal engineers of all experience levels with enough background and specific information to begin conducting thermal analysis and to participate in the thermal design of satellite systems.

1994, 581 pp, illus, Softcover, ISBN 1-884989-00-4, AIAA Members: \$59.95, List Price: \$79.95, Source: 945

Contents:

Satellite Systems Overview

Satellite Configurations
Orbits
Missions
Satellite Thermal Environments
Types of Environmental Loads
Environments in Typical Orbits
Launch/Ascent Environment
Thermal Design Examples
Spin-Stabilized Satellites
3-Axis-Stabilized Satellites
Propulsion Systems
Batteries
Antennas
Sun/Earth/Star Sensors
Cooled Devices
Solar Arrays
Systems Overview—The Hubble Space Telescope
Thermal Control Hardware
Section 1: Thermal Surface Finishes

Section 2: Mounting and Interfaces
Section 3: Multilayer Insulation and Barriers
Section 4: Heaters, Thermostats, and Solid State Controllers
Section 5: Louvers
Section 6: Radiators
Section 7: Thermoelectric Coolers
Section 8: PCMs and Heat Sinks
Section 9: Pumped Fluid Loops
Thermal Design Analysis
Satellite Project Phases
Thermal Design/Analysis Process Overview
Fundamentals of Thermal Modeling
Thermal Design Analysis Example—POAM
Margins
Thermal Math Model Computer Codes (SINDA)

Space Shuttle Integration

Engineering Compatibility
The Cargo Integration Review
Safety
Heat Pipes and Capillary Pumped Loops
Why a Heat Pipe Works
Constant-Conductance Heat Pipes
Diode Heat Pipes
Variable-Conductance Heat Pipes
Capillary Pumped Loops
Hybrid (Mechanically Assisted) Systems
Analysis
Materials
Compatibility
Testing
Heat Pipe Applications/Performance

Cryogenic Systems

Stored-Cryogen Cooling Systems
Cryogenic Radiators
Refrigerators
Design and Test Margins for Cryogenic Systems
Thermal Testing
Design Environments
Component Testing
Developmental and Subsystem Thermal Testing
Space Vehicle Thermal Tests
Factory and Launch-Site Thermal Testing
Test Techniques
Testing Checklist
One-of-a-Kind Spacecraft Thermal Testing
Technology Projections
Appendices

CA and VA residents add applicable sales tax. For shipping and handling add \$4.75 for 1-4 books (call for rates for higher quantities). All individual orders, including U.S., Canadian, and foreign, must be prepaid by personal or company check, traveler's check, international money order, or credit card (VISA, MasterCard, American Express, or Diners Club). All checks must be made payable to AIAA in U.S. dollars, drawn on a U.S. bank. Orders from libraries, corporations, government agencies, and university and college bookstores must be accompanied by an authorized purchase order. All other bookstore orders must be prepaid. Please allow 4 weeks for delivery. Prices are subject to change without notice. Returns in sellable condition will be accepted within 30 days. Sorry, we can not accept returns of case studies, conference proceedings, sale items, or software (unless defective). Non-U.S. residents are responsible for payment of any taxes required by their government.

Place your order today! Call 1-800/682-AIAA



American Institute of Aeronautics and Astronautics

Publications Customer Service, 9 Jay Gould Ct., P.O. Box 753, Waldorf, MD 20604
FAX 301/843-0159 Phone 1-800/682-2422 E-mail aiaa@tasco1.com
8 am-5 pm Eastern Standard